J Mater Sci (2010) 45:1622–1628
DOI 10.1007/s10853-009-4138-8

Improvement of high-temperature oxidation resistance of titanium-based alloy by sol–gel method

X. J. Zhang · Y. H. Gao · B. Y. Ren · N. Tsubaki

Received: 7 August 2009 / Accepted: 17 December 2009 / Published online: 30 December 2009

Abstract Sol–gel dip coating of SiO_2 was applied on a TiAl-based alloy, and subsequent heat treatment was performed. XRD and SEM/EDS analysis revealed that an amorphous silica coating was formed on the alloy. Isothermal oxidation and cyclic oxidation at 600 and 700 °C in static air of the specimens with or without coating were performed to investigate the effect of the SiO_2 coating on the oxidation behavior of the alloy by thermogravimetry. The average parabolic rate constants of the coated specimens were greatly reduced due to the presence of the coating. Severe cracks and spallation of the scales were observed on the blank specimens, but not on the coated ones. The oxide scales formed on the uncoated specimens were stratified. For the coated samples, a mixture layer of rutile TiO_2 and Al_2O_3 occurred beneath the applied film.

Introduction

Ti alloys are new kind of high-temperature structural materials applied for aerospace and aircraft industry due to their low density, high strength, and good creep resistance [1–5]. The poor ductility of Ti-based alloy at room temperature has been improved greatly by alloying and microstructure controlling. However, the poor oxidation resistance is an obstacle to its practical applications due to the formation of less protective rutile TiO_2 rather than α-Al_2O_3 scales on the surfaces occurred during exposure to high temperatures [6–9]. Thus, how to improve its high-temperature oxidation resistance has become an attracting research field.

Alloying, surface treatment, and protective coatings on the improvement of the oxygen-induced embrittlement and oxidation resistance of Ti-based alloys were widely studied. Alloying elements have been added to binary Ti–Al alloys in order to increase the oxidation resistance [6, 10–12]. The characteristic features of the scale on those alloys were the presence of a continuous Al_2O_3 layer as the second layer from the outer surface and the relatively massive precipitation of Al_2O_3 in the vicinity of the scale–metal interface [11]. The main surface treatments recently reported include silica-based enamel coating [13], aluminizing [14] and siliconizing [15–17]. Many coatings could offer oxidation protectiveness for titanium alloys and act as a barrier to reduce the ingress of oxygen at elevated temperatures [18–22]. Most of the deposited coatings usually have shortcomings of poor adhesion and significant interdiffusion [23] between the coating and the substrate. Thus, new technologies or new coating system need to be developed in order to further improve the oxidation resistance of Ti–Al-based alloys.

Sol–gel processes have been widely used to prepare various thin films for modifying the surface properties by low temperature treatment without altering the original properties of strength and toughness of the substrates [24, 25]. One of the most important advantages of the sol–gel technique is the ability to produce very small particles—usually in the nano-scale range. In our group, Al_2O_3 thin films [26, 27], Al_2O_3/ZrO_2 duplex film [28], and amorphous SiO_2 thin films [29] have been applied to improve the oxidation resistance of intermetallic compounds α_2-Ti_3Al or γ-TiAl. To our best knowledge, seldom similar

X. J. Zhang (✉) · Y. H. Gao · B. Y. Ren
College of Applied Chemistry, Shenyang University of Chemical Technology, Shenyang 110142, China
e-mail: xjzhang_syict@163.com

N. Tsubaki
Department of Applied Chemistry, School of Engineering, University of Toyama, Gofuku 3190, Toyama 930-8555, Japan

investigates were conducted on the present alloy. The aim of the present work is to prepare SiO_2 sol from TEOS raw material; the SiO_2 sol was deposited on Ti–6Al–4V alloy by a dip-coating technique, and subsequent treatment was carried out in an inert atmosphere to obtain a protective coating at high temperature, so as to investigate the effect of the SiO_2 thin film on the high-temperature oxidation resistance of Ti–6Al–4V alloy.

Experimental

SiO_2 precursor solution was prepared as the method described in Ref. [30]. First, $Si(OC_2H_5)_4$ was hydrolyzed under reflux at 70 °C for 60 min, the molar ratio of reagents was $Si(OC_2H_5)_4$:H_2O:C_2H_5OH:HCl = 1:8:5:0.05 (pH = 0.5). Second, as mentioned solution was mixed with glycol under stirring for 20 min at 60 °C. Third, cetyltrimethylammonium bromide (CTAB) was dissolved in ethanol for a concentration of 0.15 wt%. Then the ethanol solution of CTAB was added to as-prepared solution of $Si(OC_2H_5)_4$, water, C_2H_5OH, HCl, and $C_2H_6O_2$.

The commercial Ti–6Al–4V alloy was cut into specimens with dimensions 12 × 10 × 1.5 mm using a spark wire machine and their surfaces were grinded to 1000 grit SiC paper. In order to grip the specimens during the dipping coating, a hole with diameter about 2 mm was drilled. The samples were degreased ultrasonically in acetone, cleaned by distilled water and dried in air before use.

The specimens were dipped into the SiO_2 sol and withdrawn at a rate of 1 cm/min using a dip-coating equipment, dried in air for 20 min at room temperature, and then dried at 75 °C in a vacuum dry oven stove for 40 min. Heat treatment in argon atmosphere was carried out after repeating five times dipping. The level furnace was first evacuated to a pressure of 2×10^{-1} Pa and then argon was introduced as a protective gas at a flow rate of 0.5 L/min. The level furnace was then heated up to 150 °C at a rate of 5 °C/min, kept at the temperature for 1 h, and then heated up to 350 °C at the same heating rate and kept the temperature for 1 h, and finally it was heated up to 600 °C and kept the temperature for 3 h. In the present work, the specimens were dipped for 15 times and sintered for three times. The target sol–gel thin films were finally obtained by cooling the specimens to ambient temperature in the furnace. Non-treated samples were also systematically treated in all runs. After the above heat treatment, the coated alloy had a mean SiO_2 mass per unit area of 0.6 mg/cm^2. Assuming the density of silica as 2.66 g/cm^3, the calculated hypothetical SiO_2 thickness deposited on Ti–6Al–4V was 2.3 μm.

Isothermal oxidations were carried out in static air at 600 and 700 °C for 125 h with weight measurements performed at regular intervals. The specimens were placed in Al_2O_3 crucibles, oxidized at desired temperatures in ambient air, and cooled to room temperature at regular intervals of 5–20 h for mass measurement. Cyclic oxidation was also conducted at both temperatures in air in order to investigate the adhesiveness of the coating to the substrate alloy. The specimens were kept in the furnace at the desired temperature for 1 h and then taken out to cool for 20 min in air at room temperature. This process was defined as one cycle, and the cycle was repeated 100 times. An analytical balance with a sensitivity of 10^{-5} g was used to measure the mass of the specimens at intervals during the isothermal and cyclic oxidation tests.

The surface morphologies and cross-sections of the oxidized samples were characterized by scanning electronic microscope (SEM) equipped with energy dispersive spectroscopy of characteristic X-rays (EDS), while the phase compositions of the oxide scales were analyzed using an X-ray diffractometer (XRD) with Cu K_α radiation.

Results and discussion

Characteristics of the silica film

The surface and cross-sectional morphologies of the as-fabricated silica films on Ti–6Al–4V alloy were examined by SEM (see Fig. 1). The surface morphology of the film was uniform. Some pores and microcracks were observed on the surface of the thin film, attributing to the decomposition of organic component and the shrinkage of the thin film during heat treatment. Since the coatings were multilayered with every five layers fired separately, the most inner layers of the coatings were fired three times, whereas the top layers were fired only once. Therefore, the inner layers were expected to have fewer pores. Even there were pores or microcracks in the previous fired layers; these pores and microcracks would be filled at least partially by the subsequent layers of coatings due to the infiltration effect of the sol–gel dipping. Fortunately, the microcracks were not fatal because they did not penetrate the whole film, as revealed in Fig. 1b. The average thickness of the films was about 2.5 μm.

XRD patterns of the SiO_2 powders, which were prepared by heating the gel at 150, 350 °C for 1 h, and 600 °C for 3 h in succession in argon atmosphere and then grinded into powders, was characterized at 2θ = 20–85°, suggesting that the SiO_2 powders was mainly amorphous after treatment. At the same time, the coating on the Ti–6Al–4V alloy was also characterized by XRD. Its results were similar to the silica powders except for the peaks of the base alloy, as reported in Ref. [29].

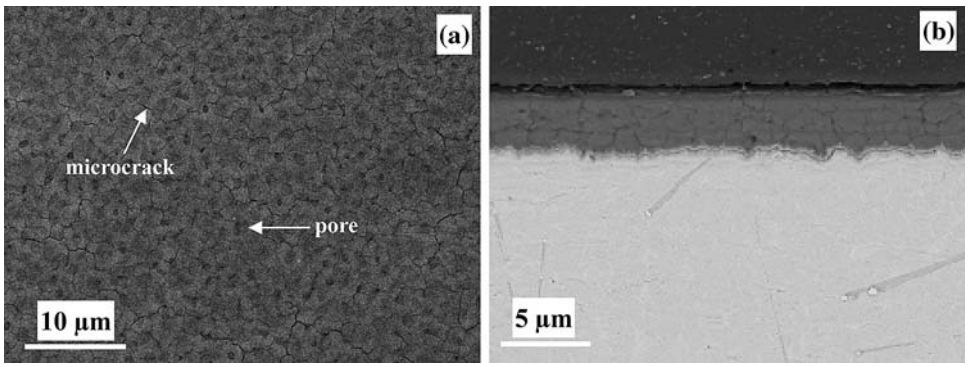

Fig. 1 Secondary electron image (**a**) and backscattered electron image (**b**) for surface and cross-sectional morphologies of the coating, respectively

Oxidation kinetics

The isothermal oxidation kinetics of the blank and coated samples was depicted in Fig. 2a, b as a function of the mass gain versus oxidation time at 600 and 700 °C, respectively. It can be seen that at the same oxidation temperature, the mass gains of the SiO_2 coated samples were much lower than those of Ti–6Al–4V-based alloy. The oxidation rate of the coated specimen at 700 °C was even slower than that of the blank alloy at 600 °C. All cases of the coated and blank specimens were deviated from the parabolic law. The fit curves for all cases were also compared in Fig. 1 so as to depict the deviation behavior. Usually, the ideal oxidation rate of an alloy or metal would obey the parabolic law when the growth of oxides is controlled by the metal ion and/or oxygen ion diffusion along the intrinsic defects. In the present cases, all deviation from the parabolic law may be attributed to the diffusion along the microcracks caused by heat and cool alternation when oxidized. The average parabolic rate constants (k_p) of the alloy and the SiO_2 coated samples could be obtained by the linear fit of $\Delta m/S = k_p t^{1/2} + A$, where S is the sample surface area (values in cm^2) and A is a constant, and k_p were listed in Table 1. It is apparent that when coated with SiO_2 film, the average parabolic rate constants of the alloy were about two orders of magnitude smaller than those for the bare alloys at both temperatures, as shown in Table 1.

Figure 3a, b showed the cyclic oxidation kinetics of the blank and coated samples in air for 100 cycles. The shape of the curve for the bare alloy at both temperatures clearly demonstrated that the characteristics of a competition between spallation and oxidation. After spallation, the fresh alloy surface was exposed to the atmosphere, thus increasing the subsequent oxidation rate. At 600 °C, spallation occurred on the bare alloy after 40 cycles. After 50 cycles, large pieces of scale began to spall off, resulting in the mass loss of the specimen. At 700 °C, severe spallation of the oxide scale occurred on the blank specimen after 25 cycles and mass gain became negative after 65 alternations of heating and cooling. Reversely, the

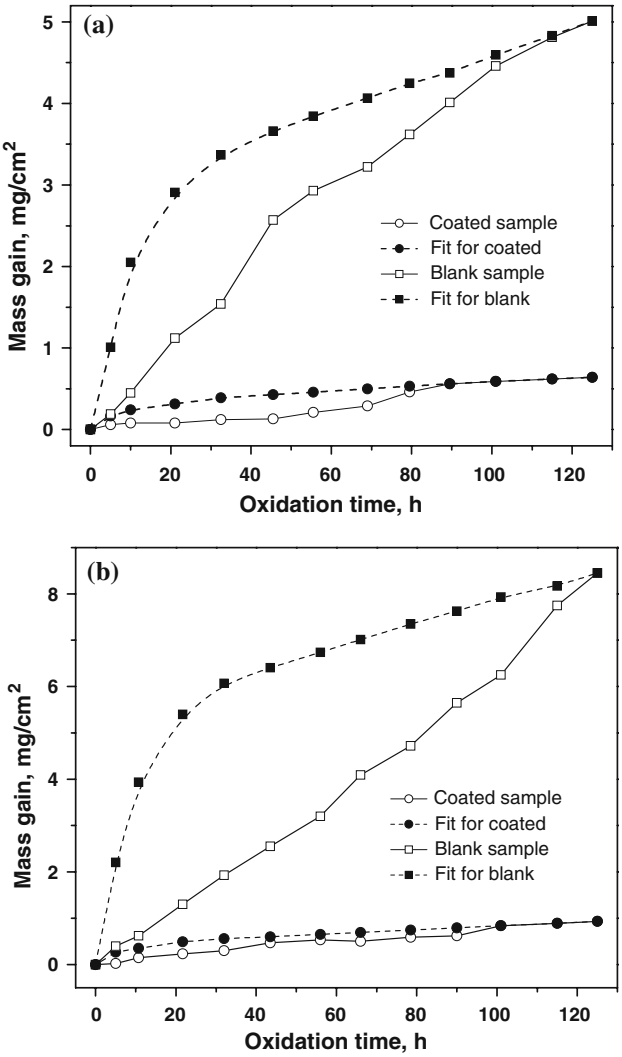

Fig. 2 Isothermal oxidation kinetics curves of the coated and blank specimens at 600 and 700 °C in air. **a** 600 °C and **b** 700 °C. The dashed is the corresponding fit curve

coated specimen had the similar oxidation kinetics to the isothermal oxidation at both temperatures. It can be seen that the mass gain of the coated specimen kept increasing during the cyclic oxidation. The oxide scale formed on the

Table 1 Average parabolic rate constants (all values in $g^2\ cm^{-4}\ s^{-1}$) for the Ti–6Al–4V with or without the silica coating oxidized in static air at 600 and 700 °C

	600 °C	700 °C
Bare alloy	3.25×10^{-11}	7.61×10^{-11}
Coated alloy	5.20×10^{-13}	1.00×10^{-12}

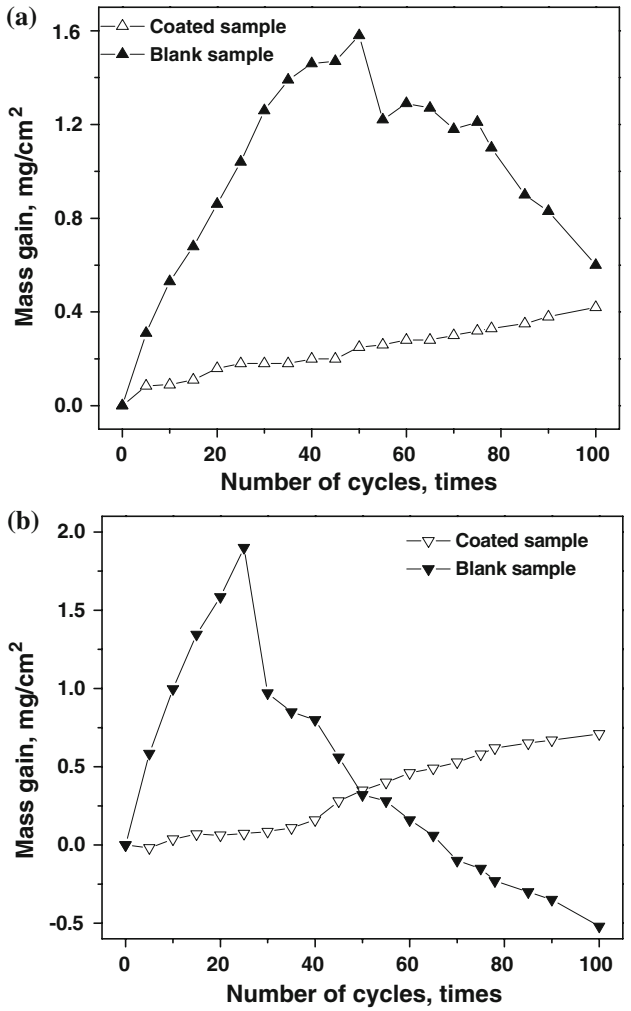

Fig. 3 Cyclic oxidation kinetics curves of the coated and blank specimens at 600 and 700 °C in air. **a** 600 °C and **b** 700 °C

coated specimen did not spall off during the whole test period, which resulted in a smooth curve.

Cyclic and isothermal oxidation tests indicated that the SiO_2 thin film significantly improved both the isothermal and cyclic oxidation resistance of the alloy at 600 and 700 °C in air.

Scale compositions

The phase compositions from XRD analysis of the oxide scales on the specimens oxidized for 125 h in air at 600 °C

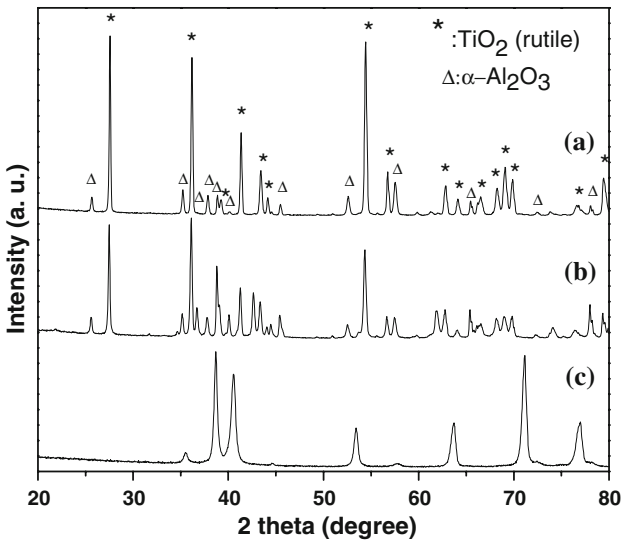

Fig. 4 XRD patterns of the samples oxidized in air for 125 h at 600 °C. (*a*) blank sample, (*b*) coated sample and (*c*) the blank sample before oxidation

were shown in Fig. 4, simultaneously, the bare specimen before oxidation was recorded to distinguish the peaks. For blank and coated specimens, the oxide scales formed on the surface were mainly rutile TiO_2. Very weak diffraction signals assigned to α-Al_2O_3 phase were also observed. No any substrate peaks were detected on the surface of the blank or coated samples.

Surface morphologies

The surface morphologies of the blank and coated specimens after 125 h isothermal oxidation at 600 °C were shown in Fig. 5, respectively. Severe cracking and spallation of the oxide scales were occurred on the bare samples, as shown in Fig. 5a, but not on the coated ones. The newly formed oxides corresponding to the TiO_2 according to the EDS microanalysis at the white net-like spots were found along some microcracks. For the coated specimens, the surface in most places maintained the original morphologies and was not covered by newly formed oxides. The spallation and cracking of the oxide scale formed on the blank specimens at 700 °C became more severe than at 600 °C. The oxide scale formed on the surface of coated specimens at 700 °C was quite similar to that observed on specimens oxidized at 600 °C.

The top views of the scales formed on specimens oxidized cyclically for 100 times were shown in Fig. 6. Severe cracking and spallation of the oxide scales were observed on the surface of the uncoated specimens at both temperatures, and the cracking and spallation became more severe with the increasing of the temperatures as well as the surface morphologies of the blank ones after isothermal

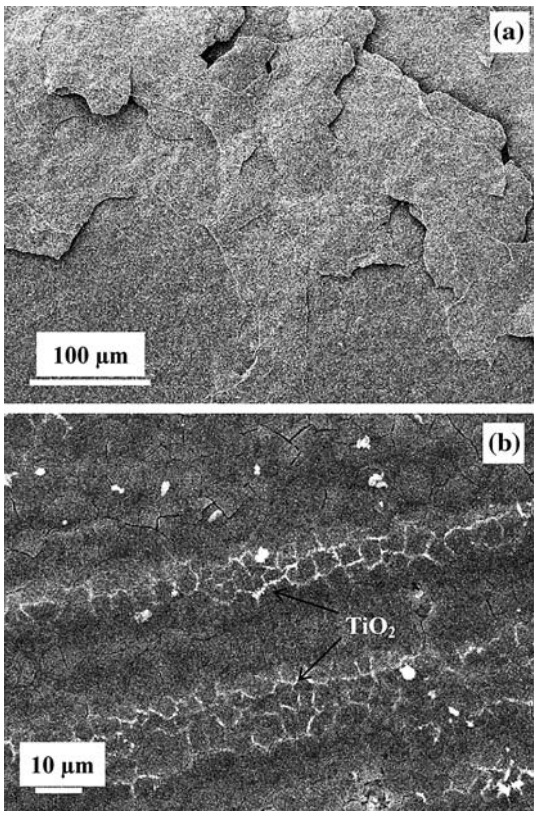

Fig. 5 Secondary electron images for the surface morphologies of blank and coated specimen after isothermal oxidation for 125 h at 600 °C. **a** Blank specimen and **b** coated one

oxidation. For the uncoated specimens, no spallation was observed at both temperatures as the cyclic oxidation kinetics curves indicated. The surface was covered with very fine newly formed oxide grain, which was corresponding to TiO_2 according the EDS results.

The cross-sectional morphologies of the specimens after isothermal oxidation for 125 h at 600 °C were shown in Fig. 6, and those at 700 °C were not shown because severe spallation of the oxide scales induced it very difficult to fix the specimens using epoxide resin. The scales formed on the coated specimens were stratified, and much thicker than that on the coated one. The layer of TiO_2 and the mixture of minor amount TiO_2 and abundant Al_2O_3 was alternating. For the coated one, the outmost layer was the applied SiO_2 thin film, following by a very thin layer composed of TiO_2 and Al_2O_3. The white layer closed to the interface between the SiO_2 coating and the oxide scale was mainly TiO_2, while the gray layer closed to the substrate was mainly Al_2O_3 according to the EDS microanalysis. The Al content at point "e" was lower than that in the substrate, suggesting that the alloy close to oxide scale was depleted in aluminum, as manifested in Fig. 7e.

Stratification of oxide scales on the bare Ti–6Al–4V alloy revealed in the present work is in agreement with previous work [31]. TiO_2 rutile phase mainly forms on the surface of Ti–6Al–4V alloy. Small amount of Al_2O_3 is present in mixture with rutile. At sufficiently high

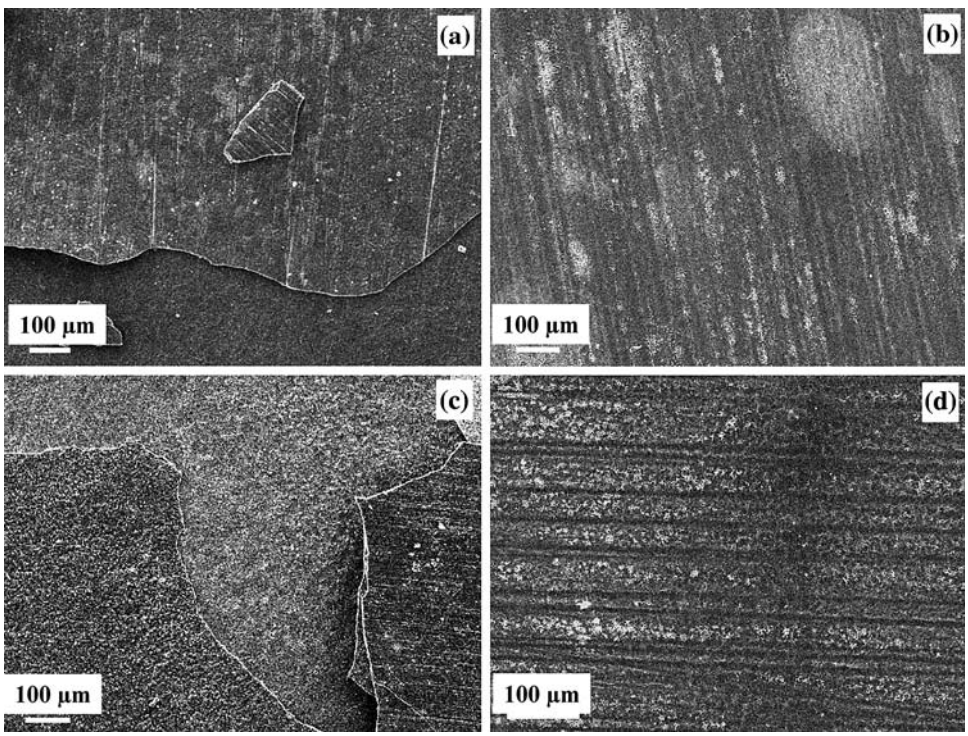

Fig. 6 Secondary electron image for the surface morphologies of blank and coated specimen after cyclic oxidation for 100 times at 600 and 700 °C. **a** Blank specimen at 600 °C, **b** coated one at 600 °C, **c** blank specimen at 700 °C, and **d** coated one at 700 °C

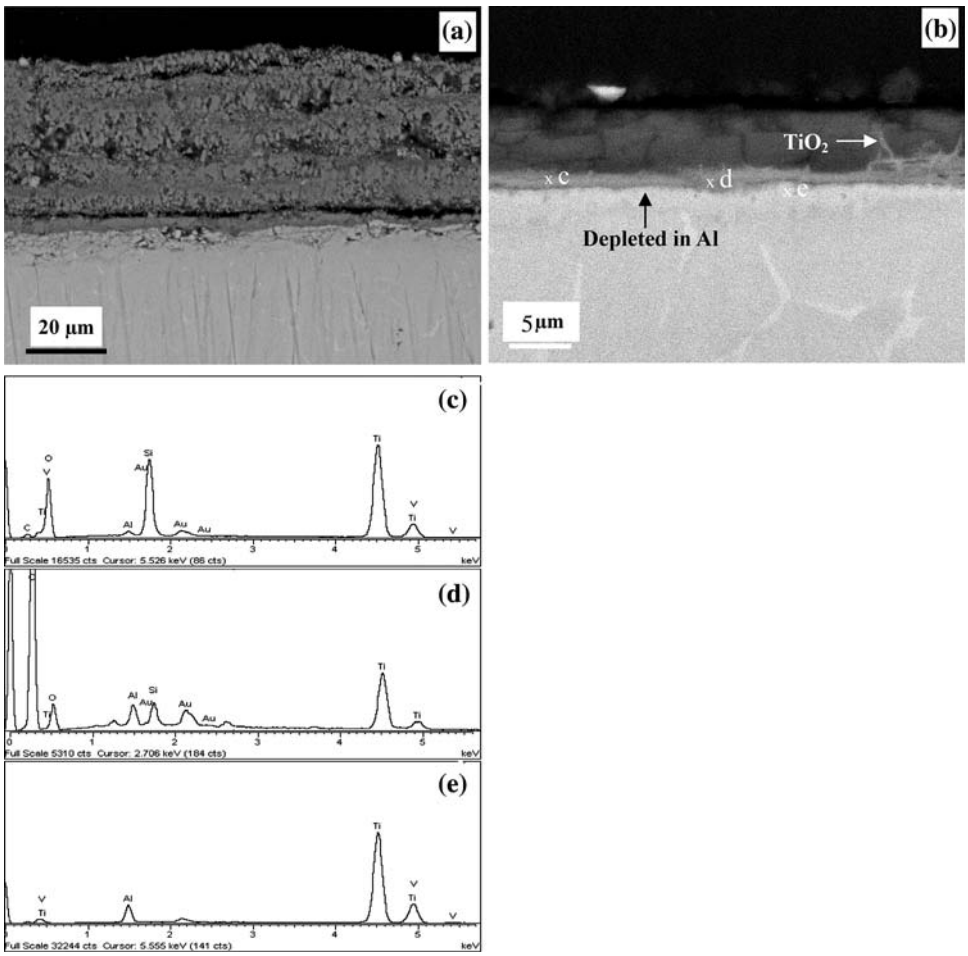

Fig. 7 Backscattered electron images for the cross-sectional morphologies of **a** blank and **b** coated specimens after 125 h oxidation at 600 °C. **c**, **d**, and **e** is the elemental composition at point "x" in image **b** by EDS analysis

temperatures, oxygen diffuses through the oxide layer, and at the metal–oxide interface, it reacts with titanium to form TiO_2. Formation of oxide layer is accompanied with the dissolution of diffusing oxygen in the metal beneath it. Increasing oxidation temperature accelerates the oxidation rate, allowing formation of thicker oxide layer and deeper oxygen diffusion zone.

Overall the results obtained in the present examination show that sol–gel SiO_2 films have beneficial effects on the oxidation resistance of Ti–6Al–4V in air at both temperatures. The present films lead to significant decrease in oxidation rates, elimination of cracking and spallation of the oxide scales during the cyclic oxidation. Under standard condition, the values of the Gibbs formation energy for Ti_2O_3 (−1433.824 kJ/mol), which transforms to TiO_2 by further oxidation, and Al_2O_3 (−1582.271 kJ/mol) in the reaction of pure Ti and Al with oxygen, respectively, are quite close [32]. The equilibrium oxygen partial pressure of TiO_2 is higher than that of Al_2O_3. Hence, the growth of TiO_2 needs high oxygen partial pressure than Al_2O_3. In addition, the oxygen pressure at the interface between the oxide scale and the substrate for the alloy/TiO_2/Al_2O_3 equilibrium is fixed under constant temperature. In view of the facts, for the coated specimens, a real possibility of the coating is that the effect of the presence of the coating reduces the oxygen pressure available at the scale surface by restricting the availability of oxygen from the gas with respect to the case of the bare alloy. In fact, in the presence of the coating oxygen has to penetrate through the coating, which may occur either by solid-state diffusion or possibly also by transport along pores, cracks, or other physical discontinuities in the coating. In any case, oxygen has a much more restricted access to the scale surface for the coated than for the uncoated samples. However, the observed reduction of the overall oxidation rate associated with an increase of the volume fraction of alumina in the mixed scales produced by the presence of the coating suggests that the reduction of the oxygen pressure at the scale surface due to the coating decreases the rate constant for the growth of TiO_2 more than that of Al_2O_3, thus favoring the formation of alumina as compared to TiO_2. As a result, the volume fraction of Al_2O_3 in the oxide scale formed on the coated specimens is more than that on uncoated one, as shown in Figs. 4 and 7. If this is correct, then a reduction of the oxygen pressure in the gas in the absence of coatings should also favor the formation of

alumina and produce a decrease of the oxidation rate of the alloy, as apparently reported in Ref. [33].

Conclusions

Sol–gel derived amorphous SiO_2 thin film has been applied on the surface of Ti–6Al–4V alloy. By investigating the isothermal and cyclic oxidation behaviors of the uncoated and coated alloys, the following conclusions can be drawn. The SiO_2 thin film had a positive effect on the oxidation resistant of the alloy. The oxidation rates were reduced at the test temperatures. Spallation and cracking of oxide scales on the bare alloy were observed, however, they were reduced on the coated ones after the deposition of silica. The relative volume fraction of Al_2O_3 on the coated specimens was greater than that on the uncoated one. The applied thin film reduced the oxygen pressure available at the scale surface by restricting the availability of oxygen from the gas in comparison with the case of the bare alloy.

References

1. Sadeghian Z, Enayati MH, Beiss P (2009) J Mater Sci 44:2566. doi:10.1007/s10853-009-3335-9
2. Cao R, Zhu H, Chen JH, Zhang J (2008) J Mater Sci 43:299. doi:10.1007/s10853-007-2172-y
3. Li YL, Feng JC, Peng H, Hua Z (2009) J Mater Sci 44:3077. doi:10.1007/s10853-009-3409-8
4. Cai JZ, Kulovits A, Shankar MR, Wiezorek J (2008) J Mater Sci 43:7474. doi:10.1007/s10853-008-2887-4
5. Liu YM, Xiu ZY, Wu GH, Yang WS, Chen GQ, Gou HS (2009) J Mater Sci 44:4258. doi:10.1007/s10853-009-3618-1
6. Rahmel A, Spencer PJ (1999) Oxid Met 35:53
7. Tetsui T (2002) Mater Sci Eng A 329–331:582
8. Yoshihara M, Kim YW (2005) Intermetallics 13:952
9. Teng LD, Nakatomi D, Seetharaman S (2007) Metall Mater Trans B38:477
10. Jiang HR, Hirohasi M, Lu Y, Imanari H (2002) Scripta Mater 46:639
11. Shida Y, Anada H (1996) Oxid Met 45:197
12. Becker S, Rahmel A, Schorr M, Schutze M (1992) Oxid Met 38:425
13. Xiong YM, Zhu SL, Wang FH (2005) Surf Coat Technol 190:195
14. Chu MS, Wu SK (2003) Acta Mater 51:3109
15. Liang W, Zhao XG (2001) Scripta Mater 44:1049
16. Xiong HP, Xie YH, Mao W, Ma WL, Chen YF, Li XH, Cheng YY (2003) Scripta Mater 49:1117
17. Li XY, Taniguchi S, Matsunaga Y (2003) Intermetallics 11:143
18. Du HL, Datta PK, Lewis DB, Burnell-Gray JS (1995) J Mater Sci 30:2640. doi:10.1007/BF00362147
19. Mckee DW, Luthra KL (1993) Surf Coat Technol 56:109
20. Clark RK, Unnan J, Wiedemann KE (1987) Oxid Met 28:391
21. Fujishiro S, Eylon D (1980) Metall Trans A: Phys Metall Mater Sci 11A:1259
22. Taniguchi S, Shibada T, Yamada T, Lou H, Wang F, Wu W (1993) Oxid Met 39:457
23. Chu MS, Wu SK (2004) Surf Coat Technol 179:257
24. Li H, Liang K, Mei L, Gu S, Wang S (2001) Mater Lett 51:320
25. Zhang S, Lee WE (2003) J Eur Ceram Soc 23:1215
26. Zhang XJ, Li Q, Zhao SY, Gao CX, Wang L, Zhang J (2008) App Sur Sci 255:1860
27. Zhu M, Li MS, Li YL, Zhou YC (2006) Mater Sci Eng A 415:177
28. Zhang XJ, Li Q, Zhao SY, Gao CX, Zhang ZG (2008) J Sol–Gel Sci Tech 47:107
29. Zhang XJ, Zhao SY, Gao CX, Wang SJ (2009) J Sol–Gel Sci Tech 49:221
30. Liu Y, Ren W, Zhang LY, Yao X (1999) Thin Solid Films 353:124
31. Sarrazin P, Coddet C (1974) Corros Sci 14:83
32. Barin I (1989) Thermochemical data of pure substrates. VCH, Weinheim
33. Kobayashi E, Yoshihara M, Tanaka R (1990) High Temp Technol 8:179